

## Liquid-salt-cooled Reactor Start-up with Natural Circulation

**Emilien Gros, Bojan Petrovic**

Georgia Institute of Technology, Nuclear and Radiological Engineering  
770 State Street, NW, Atlanta, GA 30332-0745, USA  
[emilien.gros@gatech.edu](mailto:emilien.gros@gatech.edu), [bojan.petrovic@gatech.edu](mailto:bojan.petrovic@gatech.edu)

**Davor Grgic**

University of Zagreb, School of Electrical Engineering  
Unska 3, 10000 Zagreb, Croatia  
[davor.grgic@fer.hr](mailto:davor.grgic@fer.hr)

### ABSTRACT

The Liquid-Salt-Cooled Very High-Temperature Reactor (LS-VHTR) was modeled using the neutronics analysis code SCALE6.0 and the thermal-hydraulics and kinetics modeling code RELAP5-3D with objective to devise, analyze, and evaluate the feasibility and stability of a start-up procedure for this reactor using natural circulation of the coolant and under the Loss Of Offsite Power (LOOP) conditions.

This Generation IV reactor design has been initially developed by Oak Ridge National Laboratory and studied by researchers worldwide for almost a decade. While neutronics and thermal-hydraulics analyses have been previously performed to show the performance of the reactor during normal operation and for shutdown scenarios, no study has heretofore been published to examine the active or passive start-up of the reactor.

The fuel temperature (Doppler) and coolant density coefficient of reactivity of the LS-VHTR were examined using the CSAS6 module of the SCALE6.0 code. Negative Doppler and coolant density feedback coefficients were calculated.

Two initial RELAP5 simulations were performed to obtain the steady-state conditions of the model and to predict the changes of the thermal-hydraulic parameters during the shutdown of the reactor. Next, a series of step reactivity additions to the core were simulated to determine how much reactivity can be inserted without jeopardizing the safety and stability of the core. Finally, a start-up procedure was developed, and the restart of the reactor with natural convection of the coolant was simulated. The results of the simulations demonstrated the potential for natural circulation start-up of the LS-VHTR.

### 1 INTRODUCTION

The Liquid-Salt-Cooled Very High-Temperature Reactor (LS-VHTR) is one of the six concepts of Generation IV reactors [1]. It has conceptually many promising features and combines several new technology assets such as: the use of the TRISOtopic (TRISO) fuel particles, high operating temperature ( $> 750^{\circ}\text{C}$ ), Brayton power conversion cycle, and a low pressure liquid-salt coolant. Also, it was designed with several safety features enabling passive decay heat removal: the Reactor Vessel Auxiliary Cooling System (RVACS), the Direct Reactor Auxiliary Cooling System (DRACS), and the Pool Reactor Auxiliary Cooling System (PRACS). These systems offer the capability of passively (no external power needed) removing the decay heat from the core after a shutdown. The LS-VHTR project goal is to provide an advanced design which offers the potential

for higher power output, improved efficiency of electricity production and safety, and higher operating temperatures leading to a significant reduction in plant capital costs, as well as its use in high-temperature process heat applications.

Regulations for current nuclear power plants demand that a nuclear power plant have redundant safety features, including two connections to the electrical grid. In case of a loss of offsite power (LOOP), during a blackout for instance, the plant loses these connections, and may have to be tripped for safety reasons. After a power outage, since nuclear power plants require re-establishing the two connections and a large amount of energy to be started-up, they are usually the last power stations to be brought back on-line, leading to significant economic losses.

This paper evaluates the feasibility and stability of a start-up process for the LS-VHTR with natural circulation of the coolant. This novel concept for the start-up of a nuclear plant of LS-VHTR type would enable the restart of the plant under LOOP conditions, which would then help to restore the grid.

Limited experience related to start-up and operation under natural circulation of the coolant comes from the Dodewaard nuclear power plant, that was operated in the Netherlands until 1997, with a net output of 55 MWe [2], and from the passively safe generation III+ reactor ESBWR (Economic Simplified Boiling Water Reactor) designed by GE Hitachi Nuclear Energy that is waiting for final design certification [3]. However, the Dodewaard reactor and the ESBWR are Boiling Water Reactors (BWRs), thus physics phenomena are different than in the LS-VHTR.

## 2 LSCR SUMMARY

The LS-VHTR represents a unique merging of several design features. In this chapter, the specifics of the design chosen are presented.

### 2.1 Configuration, fuel element, fuel assembly and fuel core design

A functional diagram of the LS-VHTR layout is shown in Figure 1. The core and the primary heat exchanger are located in a large pool containing a buffer salt. The heat generated by the fuel is removed by a liquid-salt coolant flowing upwards through the core. This fluid flows in a primary loop through the primary heat exchanger, where heat is transferred to an intermediate loop containing another salt. The primary loop is closed and immersed in the buffer salt tank. The salt in the secondary loop conveys heat to a second heat exchanger, where helium flowing in a third loop is heated. This helium, once heated, flows through turbines in order to produce electricity. Alternatively, supercritical CO<sub>2</sub> or supercritical steam may be used.

The core is 12 m tall, and is composed of 8 m of active fuel, a lower plenum, lower reflector, upper reflector, and upper plenum of 1 m height each. The core diameter (including fuel assemblies and outer reflector blocks) is 9.2 m.

The LS-VHTR uses TRISO (TRiISOtopic) fuel particles, which were developed for use in various high temperature reactor concepts. It consists of a fuel kernel made of uranium oxycarbide (UCO) or uranium dioxide (UO<sub>2</sub>), surrounded by four different layers of carbon and silicon carbide.

The prismatic block fuel assembly option is considered in this study. A single fuel block is shown in Figure 2. It has a flat-to-flat dimension of 36 cm, is 79.3 cm high, and is made of graphite. One fuel block contains 216 fuel channels (1.27 cm diameter) and 108 coolant channels (0.953 cm diameter). The fuel and coolant channels are arranged in a triangular array.

The reactor core layout is shown in Figure 2. The core has a diameter of 9 m. It consists of 265 fuel assemblies arranged so that they form a fuel region surrounded by four rows of reflector blocks. The latter have the same dimensions as the fuel blocks, and are composed of graphite.

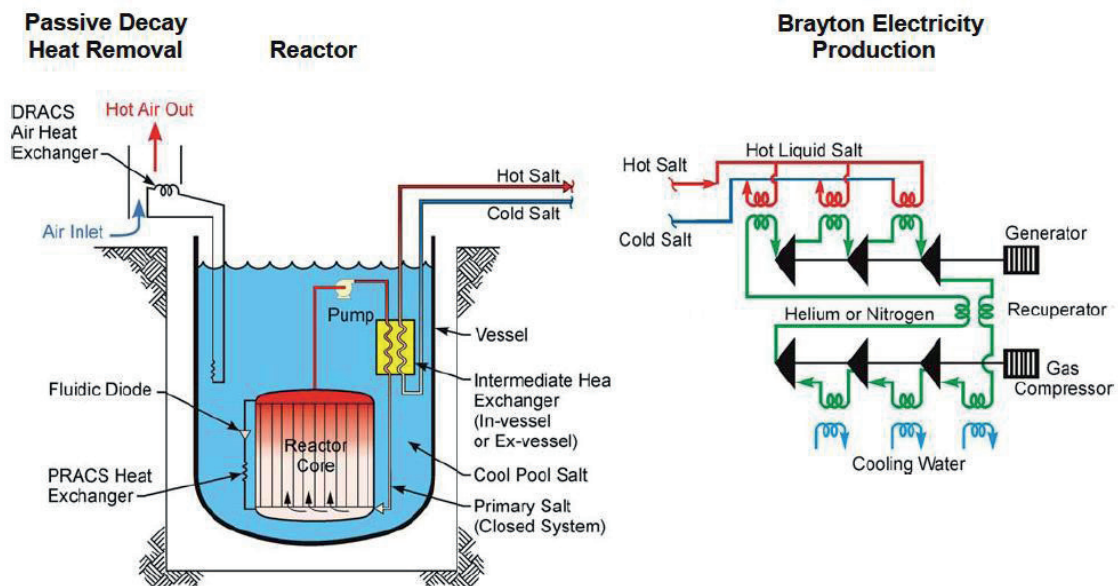


Figure 1: Configuration of the LS-VHTR plant [4]

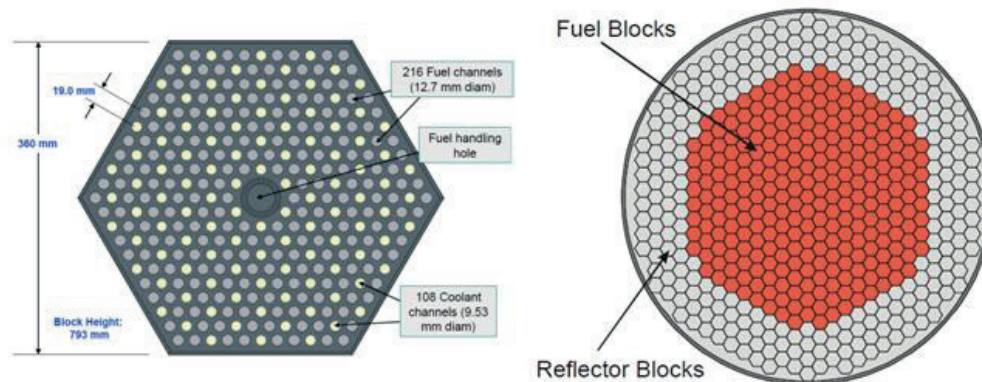


Figure 2: LS-VHTR hexagonal fuel assembly block [5] and reactor core layout [6]

## 2.2

### Salt choice

There are several salts under consideration for use in the LS-VHTR such as:  $\text{LiF-BeF}_2$  (FLiBe),  $\text{NaFBeF}_2$ ,  $\text{LiF-NaF-KF}$  (FLiNaK), or  $\text{NaF-ZrF}_4$  [4]. Salts are used for heat transport in this reactor. They are characterized by high boiling point, good heat transfer capabilities, and they enable the reactor to be operated at high temperatures. These characteristics lead to higher power efficiencies. Based on attractive neutronics as well as other properties including heat transfer characteristics, material compatibility, freezing temperature, cost and other criteria, FLiBe is usually preferred to other candidates to be the primary salt [6]. FLiNaK is considered as a good candidate for the intermediate loop [4], and was chosen as the intermediate salt in this study.

FLiBe is a compound of LiF (66%) and  $\text{BeF}_2$  (34%). It has a relatively low neutron absorption cross section. FLiBe salt shows great performance under activation; it does not generate gamma activity for more than one minute past being activated. Finally, the melting temperature of FLiBe is  $459^\circ\text{C}$ , and its boiling temperature is  $1430^\circ\text{C}$  [7].

FLiNaK is a compound of LiF (46.5%), NaF (11.5%) and KF (42%). It has a similar freezing point as FLiBe, but a lower heat capacity, lower thermal conductivity, and higher neutron absorption cross section. The melting and boiling temperature of FLiNaK are  $454^\circ\text{C}$  and  $1570^\circ\text{C}$  respectively [8]. FLiNaK is also cheaper than FLiBe [9].

### 3 METHODOLOGY

To evaluate the start-up of the LS-VHTR with natural circulation of the coolant, the neutronics and thermal-hydraulic aspects of the reactor have been studied. The CSAS6 [10] package of SCALE6.0 [11] was used to perform neutronic calculations. The thermal-hydraulics and kinetics calculations and simulations were done by employing the RELAP5-3D [12] code. The methodology developed to simulate the start-up of the reactor was as follows.

A 3-dimensional model of one fuel assembly of the LS-VHTR core was developed in SCALE6.0. Several simulations were run with different fuel temperatures to calculate the temperature reactivity feedback of the fuel assembly. The density of the coolant was then varied from  $1.80 \text{ g/cm}^3$  to  $2.05 \text{ g/cm}^3$  to get the coolant density reactivity dependency of the fuel assembly. Given that the fuel temperature feedback and the coolant density feedback of the entire core of the reactor are expected to be similar, it was decided to make the simulations on the fuel assembly only, with proper boundary conditions.

In this study, we are essentially interested in understanding how the temperature, pressure and flow in the primary loop and power profiles in the core would change during the start-up. Thus, only the primary loop and the intermediate loop of the nuclear power plant layout (see Figure 1) were modeled with the RELAP5 code. The primary loop, with FLiBe flowing through, was modeled as a closed loop in order to get as realistic results as possible. Only the heat exchanger of the intermediate loop was accurately modeled, the inlet and the outlet of the heat exchanger were treated as boundary conditions. Fuel temperature and coolant density feedback from the neutronic calculations were entered in the RELAP5 model as an input. RELAP5 was used to simulate three phases: normal operation, shutdown, and start-up. The reactor operation under steady-state conditions was first simulated. The shutdown of the reactor was then simulated using initial conditions from the previous simulation. Finally, using the reactivity feedbacks from the neutronics code, the thermal-hydraulic initial conditions from the shutdown simulation, and specifying a set of reactivity insertion steps the start-up of the LS-VHTR plant was simulated. This paper focuses on the results of the start-up simulation.

### 4 CORE PHYSICS

#### 4.1 SCALE6.0 model

The effort to analyze the reactivity changes with respect to fuel temperature and coolant density is performed by modeling the reactor fuel assembly in the Standardized Computer Analyses for Licensing Evaluation Modular Code System (SCALE6.0). The SCALE system was developed by ORNL and is capable of performing criticality, shielding, spent fuel depletion or decay, and reactor physics calculations [13]. All calculations were done using the Criticality Safety Analysis Sequence (CSAS6) with KENO-VI [14] package of the SCALE6.0 code. It was decided to use fresh fuel everywhere in the fuel assembly for simplicity. Also, all of the calculations were made at the beginning of life of the fuel, which is 10% enriched in  $\text{U}^{235}$ . Future work should reexamine these coefficients for different fuel enrichment and burnups.

The three main materials encountered in the LS-VHTR core and modeled in SCALE6.0 are the fuel, the coolant, and the graphite used in the upper, lower and radial reflectors, and in the graphite blocks.

The TRISO fuel particles were modeled with the double-heterogeneity option of SCALE. The fuel kernel, graphite, and SiC layers composition were defined according to the specifications provided by ORNL. Silicon carbide is defined as a special mixture with the natural isotopic abundance of Silicon ( $^{28}\text{Si} = 92.23\%$ ,  $^{29}\text{Si} = 4.67\%$ , and  $^{30}\text{Si} = 3.1\%$ ). The TRISO particle volume fraction was set to 0.30 based on the range of values considered in literature.

The primary coolant composition, FLiBe (66% LiF, 34%  $\text{BeF}_2$ ), was also described as a weight percent mixture of its isotopic components. The lithium in FLiBe was assumed to be

enriched to 99.99% in  $^7\text{Li}$ , given that it is difficult to produce Lithium with less than 0.01% of  $^6\text{Li}$  [5].

Instead of modeling the actual reactivity control system, it was decided to mix boron with the graphite of the fuel assembly blocks and reflectors in order to get a multiplication factor around 1. Thus, a weight percent mixture of graphite and  $^{10}\text{B}$  (99.9985% and 0.0015%) with a density of  $1.74\text{ g/cm}^3$  was defined for the material of the fuel assembly blocks and of the reflectors.

To accurately model the triangular pitch of the fuel assembly design, hexagonal lattice geometry was used to describe the fuel, coolant and graphite blocks. The fuel and coolant units are defined as a cylindrical form filled with fuel or FLiBe inserted in a hexagonal graphite block. These units were placed in an array to reproduce the pattern shown in Figure 2.

Mirror boundary conditions were set on the outer limit of the hexagon modeling the fuel assembly block, simulating the effect of the large core. This enabled us to make the calculations on the fuel assembly level and to assume that the results are similar to that we would obtain by simulating the whole core.

## 4.2 Results

To get enough statistical precision on the multiplication factor, KENO-VI simulations were performed using 1,000 generations with 10,000 neutrons per generation. This resulted in a  $1\sigma$  statistical uncertainty ranging from  $1.4 \cdot 10^{-4}$  to  $1.9 \cdot 10^{-4}$ .

For the Doppler coefficient calculation, simulations were run with a coolant temperature of 1143 K, which is the temperature of the coolant right before the reactor is started-up. Seven simulations were run with fuel temperatures ranging from 873 K to 1473 K. The reactivity value ( $\rho$ ) was calculated from the neutron multiplication factor value. The RELAP5 code requires that the reactivity be entered in dollars (\$) in the kinetics input. Thus, the value of the reactivity in dk/k unit was divided by the effective delayed neutron fraction ( $\beta = 0.0065$ ) to convert it into \$ units. The results were arranged in a table and plotted. The equation of the relation between reactivity and fuel temperature ( $\rho = \text{func}(\text{TF})$ ) were  $\text{func}$  is a function of the fuel temperature, TF) was extracted from this plot. The value of the derivative of this relation with respect to fuel temperature was finally calculated at different fuel temperatures to get the Doppler temperature coefficient of reactivity. The results of the CSAS6 simulations are presented in Figure 3.

The calculated Doppler fuel temperature coefficient of the core is  $-\$0.0074/\text{K}$ . This value is in acceptable agreement with the temperature coefficient estimated by ORNL for the AHTR:  $-\$0.01/\text{K}$  [5].

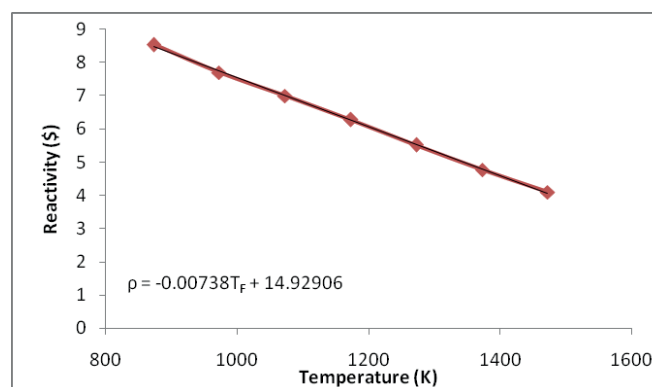


Figure 3: Calculated reactivity for 7 different fuel temperatures

For the coolant density reactivity coefficient calculation, the fuel temperature was set to 1150 K for all the simulations and the coolant temperature to 1140 K. These temperatures correspond to the average temperature in the fuel and coolant before the reactor is started-up.

Simulations were run for six different FLiBe densities, ranging from 1.60 g/cm<sup>3</sup> to 2.15 g/cm<sup>3</sup>. Results and plots of the simulations are given in Figure 4.

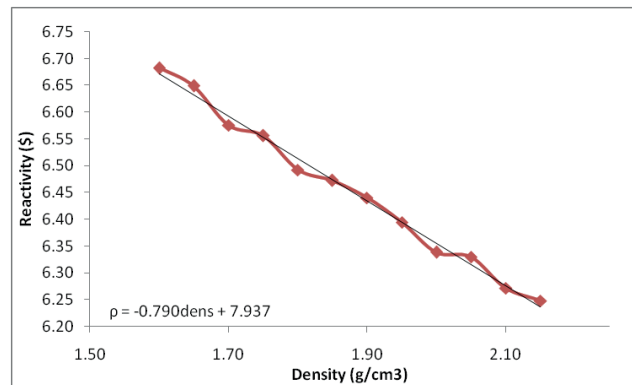


Figure 4: Calculated reactivity for 12 different coolant densities

The reactivity of the system decreases with increasing coolant densities. Given that an increase in coolant temperature results in a decrease of the coolant density, an increase in FLiBe temperature would lead to an increase of the reactivity of the system. This could lead to instabilities; however, for a coolant density change of 0.25 g/cm<sup>3</sup>, the reactivity decreases from \$6.68 to \$6.47, i.e., only ~\$0.2. The following correlation, Eq. (1), was used for the FLiBe density with respect to temperature [15]:

$$\rho_{\text{FLiBe}} = A_D (T_{\text{FLiBe}} - 273.15) + B_D \quad (1)$$

With  $A_D = -0.4884 \text{ kg/m}^3/\text{K}$ , and  $B_D = 2279.7 \text{ kg/m}^3$ , it was calculated that densities ranging from 1.80 g/cm<sup>3</sup> to 2.05 g/cm<sup>3</sup> correspond to temperatures ranging from 1250 K to 750 K. Thus, a coolant density decrease of 0.25 g/cm<sup>3</sup>, corresponding to a coolant temperature increase of 500 K, would lead to about \$0.2 reactivity insertion. This effect is small, considering that during the start-up of the reactor, the temperature increase rate is usually on the order of magnitude of 50 K/hr. In addition, an increase in temperature also leads to a negative fuel temperature feedback that is much larger than the density feedback.

### 4.3 Radial and axial power distribution

The radial power distribution profile was established based on ORNL’s calculations, done with MCNP and a 10-ring core model [6]. These 10 rings were grouped to form three radial regions across the core, as illustrated in Figure 4.

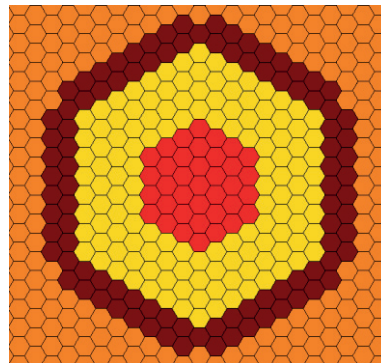


Figure 5: Inner, middle, and outer region of the LS-VHTR core

The inner region groups the rings 1, 2, 3 and 4. The rings 5, 6, 7 and 8 constitute the middle region. The outer region is composed of the two outer rows of fuel assemblies; rings 9 and 10. A

summary of the characteristics of the groups is given in Table 1. One can observe that the inner group produces more power per fuel assembly than the outer group.

	Group 1 (inner)	Group 2 (middle)	Group 3 (outer)
Number of assemblies in the region	37	132	96
Fraction of total number of assemblies	14%	50%	36%
Power generated by the region	446.04 MW	1278.34 MW	673.80 MW
Fraction of total power	18.60%	53.30%	28.10%
Peak to average factor	1.33	1.07	0.78

Table 1: Description of the model core regions

The axial power distribution profile is used by RELAP to calculate the heat transferred to the coolant channels in each axial segment modeling the core. An internal source multiplier value was specified for each axial segment of the three heat structures modeling the fuel channels of the three rings of the core. These values are multiplied by the total power (specified manually or calculated with the point reactor kinetics equations) to obtain the power generated in the heat structure [16]. The axial power profile chosen is based on a profile used by ORNL to model the LS-VHTR [6]. This axial distribution was also used for gas-cooled VHTR modeling [17]. The power profile that was chosen is shown in Figure 6. To get the power profile in each region of the core, the distribution of Figure 6 was multiplied by the power generated in every region, as specified in Table 1. The axial power distribution obtained for each group of fuel assemblies is shown in Figure 7.

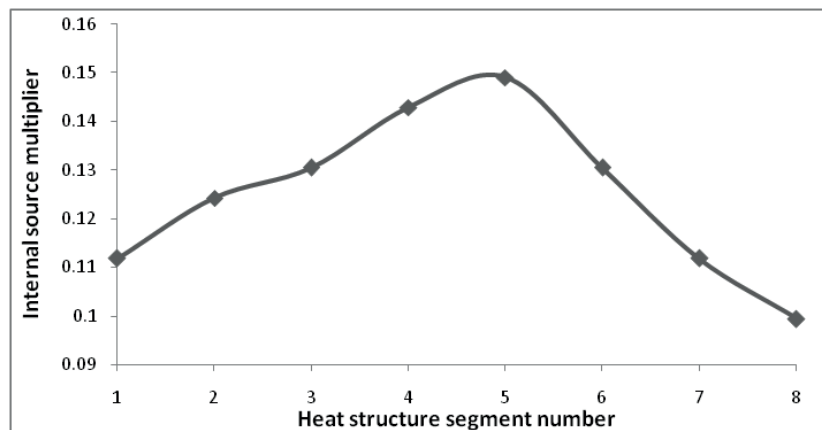


Figure 6: Representative axial power distribution profile

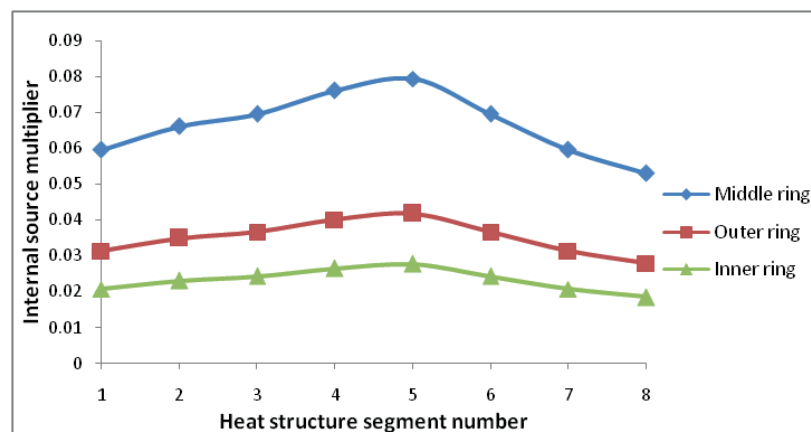


Figure 7: Axial power distribution profile in the core regions

## 5 RELAP5 NODALIZATION/MODEL

Thermal-hydraulics analyses were performed using the Reactor Excursion and Leak Analysis Program (RELAP), developed at the Idaho National Laboratory (INL), which offers the capability to calculate the behavior of a reactor coolant system and the reactor kinetics during a transient. The RELAP5 code has been originally developed to model Light Water Reactors (LWRs). Though, the properties of several molten salts including FLiBe and FLiNaK have been subsequently incorporated [15], making the modeling of the LS-VHTR possible. The heat transfer coefficients used by RELAP5 for reactors with a salt coolant are the same as that used in the code to model LWRs, however, it was shown experimentally that this was an acceptable approximation.

### 5.1 Nodalization, hydrodynamic components and main parameters

The model encompasses the core, the primary coolant (FLiBe) loop, two IHXs, and part of the intermediate coolant loop. The primary salt flows upwards through the core and downwards through the shell side of the IHX. The secondary coolant (FLiNaK) flows upwards through the tube side of the IHX. A schematic of the RELAP5 model is given in Figure 8. The components 10, 20 and 30 represent the coolant channels, corresponding to three core regions (inner, middle, outer). The core has been divided radially in three groups of fuel assemblies to increase the fidelity of the model. The core is divided into 8 segments axially. For example, for the component 10, segments 1 through 8 model the same fuel assemblies at different elevations.

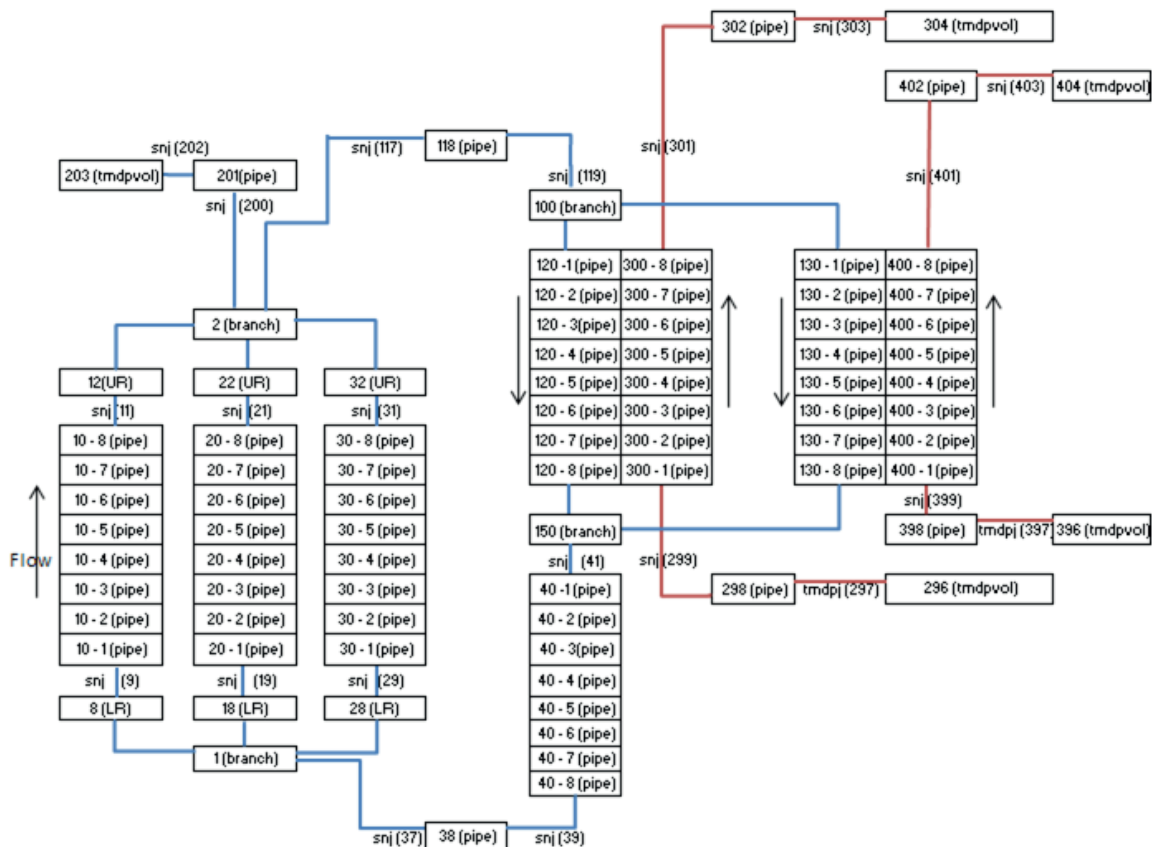


Figure 8: RELAP5 model of a LS-VHTR

The lower and upper reflectors are represented by the components 8, 18, 28 and 12, 22, 32 respectively. Given that the bypass flow in radial reflectors is assumed negligible (less than 5%), the radial reflectors were not modeled. Components 1 and 2 represent the lower and upper plenum



respectively. The pipe 201 and the time dependent volume 203 model the pressure maintenance system above the upper plenum. The pipes 118 and 38 make the connection between the upper plenum and the upper header of the IHXs (component 100) at the top, and between the downcomer (component 40) and the lower plenum at the bottom. Components 100 and 150 represent the upper head and lower head of the IHXs. Components 120 and 130 represent the shell side of the IHXs, while components 300 and 400 represent the tube side of the IHXs. Components 296, 298, 302 and 304, 396, 398, 402 and 404 represent the secondary loop. Boundary conditions were specified in the junctions 297 and 397, in order to force the flow of the secondary loop.

The basic core design values are as follows in the RELAP5 model:

- Graphite block: 36 cm flat-to-flat, 8 m height
- Fuel cylinder modeling the fuel kernels of the TRISO particles: 0.6762 cm diameter
- Coolant channel: 0.953 cm diameter
- Core: 265 fuel assemblies
- Primary coolant: FLiBe (2LiF-BeF<sub>2</sub>)
- Primary coolant expected steady-state temperatures: 1173 K inlet, 1273 K outlet
- Thermal power: 2400 MW
- Core flow: 10,000 kg/s

The dimensions and main parameters assumed for the other components are listed below:

- Top and bottom reflectors: 1 m thick, same flow area as coolant channels
- Upper and lower plenums: 2 m and 1 m height respectively, same flow area as the core
- Heat exchanger: shell and tube heat exchanger
- Intermediate loop flow: 16,400 kg/s
- Intermediate loop steady state temperatures: 1140 K inlet, 1200 K outlet

The flow areas and length of the primary loop components were defined as follows:

- Plenum flow area: 2.032 m<sup>2</sup>
- Inner assembly ring flow area and height: 0.284 m<sup>2</sup>, 8 m
- Middle assembly ring flow area and height: 1.01 m<sup>2</sup>, 8 m
- Outer assembly ring flow area and height: 0.736 m<sup>2</sup>, 8 m
- Transport pipe flow area and length: 0.5 m<sup>2</sup>, 2 m
- Downcomer flow area and length: 0.5 m<sup>2</sup>, 3.2 m

The material properties (specific volumetric heat capacity and thermal conductivity) used in the analyses are as follows:

- Fuel:  $c_p = 2.76e6 \text{ J/m}^3\text{K}$ ,  $k = 10.0 \text{ W/mK}$  [4]
- Graphite blocks:  $c_p = 3.276e6 \text{ J/m}^3\text{K}$ ,  $k = 30.0 \text{ W/mK}$  [4]
- Coolant salt, FLiBe:  $c_p = 4.39e6 \text{ J/m}^3\text{K}$ ,  $k = 1.1 \text{ W/mK}$  [4]
- Hastelloy N alloy:  $c_p = 5.12e6 \text{ J/m}^3\text{K}$ ,  $k = 23.6 \text{ W/mK}$  [18]

## 5.2 Heat structures

Several heat structures have been defined in the model, attached to the coolant channels, the upper and lower reflectors, and the heat exchanger.

One heat structure has been implemented for each ring of the core (10, 20 and 30) to model the heat transferred to the coolant channels via the power generated by the fuel. The fuel heat structures are cylindrical, and their outer boundary is attached to the corresponding coolant channel hydrodynamic component. The RELAP5 code offers the capability to model a simple fuel configuration only. For instance, the following type of fuel structure can be modeled in RELAP5: a cylindrical fuel rod surrounded by a cladding layer and an external layer of another material. The coolant channel is connected to the heat structure as a boundary condition. The fuel used in the LS-VHTR is a fuel compact, made of TRISO fuel particles assembled together in a graphite moderating matrix. Finding a model that would exactly reproduce the TRISO fuel performance was intricate.

Thus, assumptions were made to approximate heat transfer as much as possible. The fuel heat structure model is as follows:

- One cylindrical rod was defined to model the fuel
- A layer of graphite was set around the fuel to model the TRISO particle outer carbide layers, the graphite moderating matrix of the compact, and the graphite of the fuel assembly blocks

The radius of the rod modeling the fuel was calculated using the proportion of fuel in the TRISO particles (fuel kernel size) and the proportion of TRISO particles in the fuel compact (packing fraction). The calculated radius of the fuel rod is:  $3.3771 \cdot 10^{-3}$  cm. One should note that this may not be the most accurate way to model the performance of the TRISO particles with the RELAP5 code. Though, since this study aims at providing a model to evaluate the stability and feasibility of a start-up procedure with natural circulation, it was decided that this modeling of the fuel was the only practical option and adequate for the objectives. Further work is needed to provide a more realistic model of the TRISO fuel, but this was out of the scope of this work.

Six heat structures have been defined to model the lower and upper reflectors. These heat structures are similar to the fuel heat structure, except that the material is graphite.

Each heat exchanger has an associated heat structure. The latter consists of a cylindrical layer of Hastelloy N alloy, with the secondary loop as the inner boundary (tube side of the IHX) and the primary loop as the outer boundary (shell side of the IHX). For simplicity, it was decided not to model the baffles. The heat structure as presented models a simple straight-tube shell-and-tube type heat exchanger.

The heat losses in the plenums are assumed negligible. Thus, no additional heat structure has been defined.

### 5.3 Form loss coefficients

Given that the start-up of the LS-VHTR under natural circulation was studied, it was essential to take the flow resistance in the loop into account. To do so, form loss coefficients were specified to model the friction losses due to the abrupt area changes at the entrance of the lower axial reflectors and at the exit of the upper axial reflectors. Form loss coefficients were also specified at the entrance and the exit of the heat exchanger. Each loss coefficient was assumed to be 0.25, based on the typical loss coefficient used in LS-VHTR RELAP5 model [6]. In this study, the pump was not modeled with the RELAP5 component “pump”. Instead, a time-dependant junction was used (junction 117 in Figure 8) to force the flow during steady-state conditions operation, and a simple junction was used to let RELAP5 calculate the flow during operation with natural circulation of the salt in the primary loop. A form loss coefficient of 1.0 was entered in the junction modeling the pump (in active or passive mode) to account for the pressure drop induced. This form loss coefficient was assumed; thus, the behavior of the pump as modeled might differ from the behavior of the actual pump in the LS-VHTR design. This assumption impacts the value of the natural circulation mass flow rates predicted by the RELAP5 code and should be taken into account when observing the results of the different simulations that will be presented later in this paper.

## 6 SIMULATIONS AND RESULTS

To model the start-up of the reactor under natural circulation of the coolant, the kinetics mode of RELAP5 was used to calculate the power and reactivity changes of the core during the transient. The flow in the different rings of the core was also calculated by the program. The initial temperature, pressure and flow conditions are set to the final values obtained at the end of a shutdown simulation, which is not presented in this paper. The initial power consists of only decay power, and is set to about 21.5 MW by specifying a power history table in the input file.

## 6.1 \$0.15 step reactivity insertion simulation

In this simulation, \$0.15 of reactivity is inserted at  $t = 100$  s. The initial 100 s before inserting the reactivity rather than doing it at time  $t = 0$  s is intended to allow the code to reach a steady state with the kinetics mode activated. Figure 9 shows the changes in reactivity, total power, decay, and fission power respectively during the transient that follows the insertion of reactivity in the core.

The positive reactivity is inserted at  $t = 100$  s, while the power swing occurs only after 1500 s. This can be explained by the prompt jump approximation [19]. In this approximation, the fission power is initially increased by the factor:  $\beta / (\beta - \rho)$ , where  $\rho$  is the reactivity inserted. Then, the fission power increases exponentially by the factor  $e$  in magnitude every reactor period. Given that the initial fission power equals  $2.15 \times 10^{-5}$  W, it takes a certain time for the fission power to increase to significant values even if the increase is exponential. That initial value of the fission power was calculated by RELAP5, based on the power history table that was entered, and thus may differ from the actual value of fission power in the LS-VHTR eight hours after a shutdown from full power condition. The total core reactivity goes to \$0.15 after the insertion and remains at this value for about 1500 s. After this time, due to the feedback, the total core reactivity oscillates to stabilize again at its initial \$0 value at  $t = 3000$  s. Thus, it takes less than an hour for the core to stabilize after a \$0.15 positive reactivity insertion. The decay power slowly decreases until 1500 s, since no significant new fission occurs, and then increases because of the new fissions happening in the core. The results plotted show that the power level is increased from 21.5 MW to 98.5 MW. The core inlet, outlet, and fuel centerline peak temperature are at the time  $t = 4500$  s: 1133.6, 1186.1 and 1191.8 K. The mass flow driven by natural convection is increased from 474.2 kg/s initially to 785.7 kg/s at the end of the simulation.

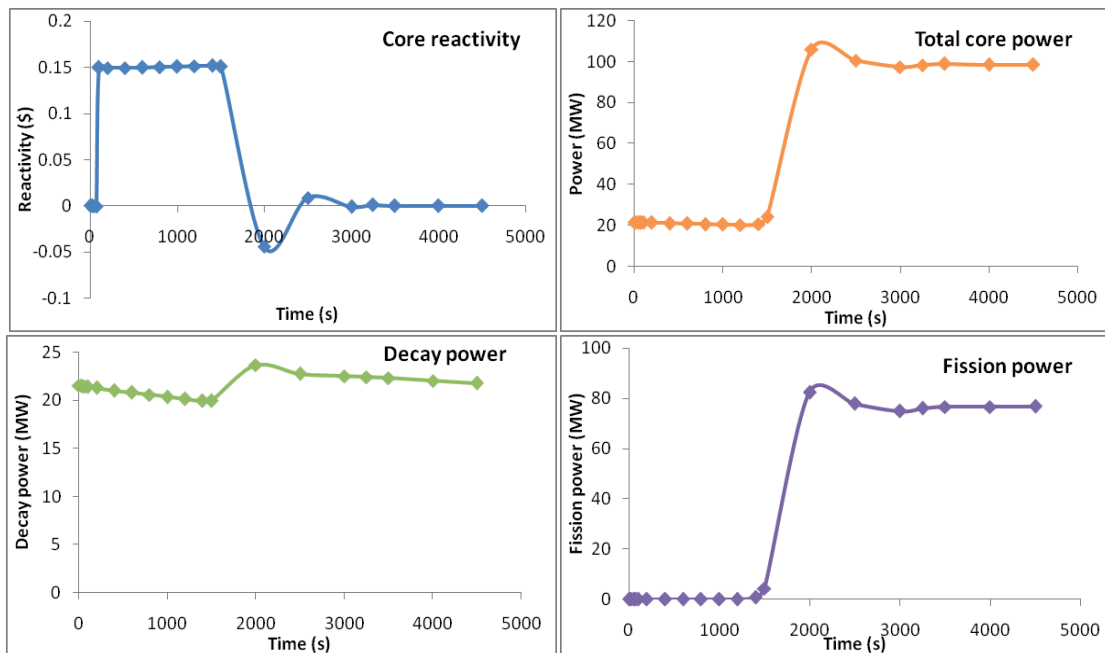


Figure 9: Changes in reactivity, total power, decay power, and fission power over time

In order to provide a thorough understanding of the phenomena happening during the transient following the control rods removal, other thermal-hydraulic parameter values were plotted in Figure 10.

The effect of the reactivity insertion on the flow and temperatures in the inner, middle and outer rings of the core can be seen after 1500 s. Due to the significant power increase, the outlet and inlet temperatures are increased. The outlet temperature increase equals about 38 K in the three core regions. Though, the temperature increase in the first axial segment of the inner region is twice as high as the increase in the inner or middle assemblies. This leads to a lower temperature differential

in the outer region of the core than in the inner and middle region. As a consequence of the varying temperature increases, the coolant behaves differently in each region of the core. Figure 5.27 shows that from  $t = 1200$  s to  $t = 1800$  s the mass flow in the outer fuel assembly ring decreases. This decrease is due to the natural circulation of the coolant, and should be kept limited to avoid counter-flow.

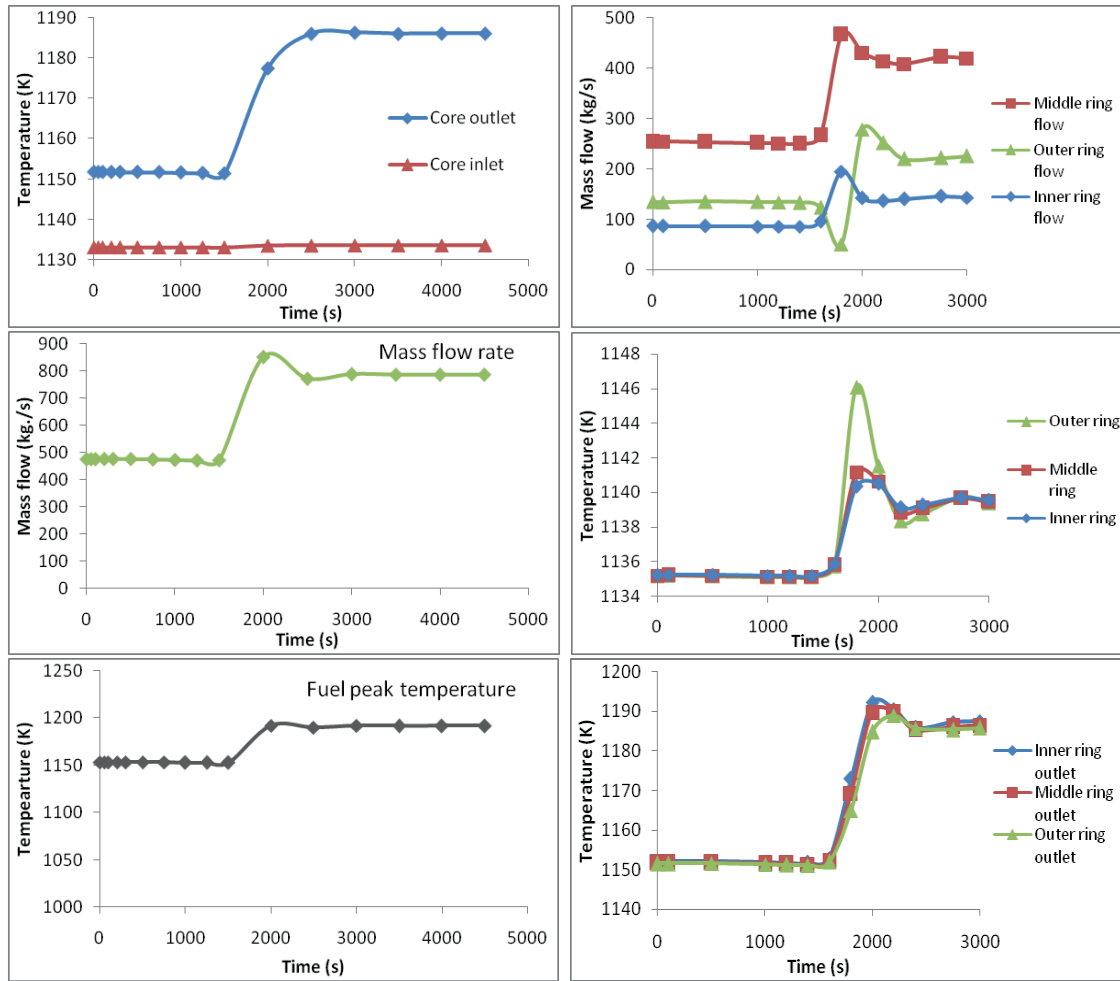


Figure 10: Changes in core outlet and inlet temperature, mass flow rate, fuel peak temperature, core mass flow rates, bottom of core temperature, and core outlet temperature

## 6.2 Summary of single step reactivity insertion simulations

Analysis for eight different single step reactivity insertions was performed, analogous to the \$0.15 insertion. The results of are summarized and presented in Table 2.

Reactivity inserted (\$)	Final Power (MW)	Fraction of total power achieved	Peak fuel temperature (K)	Negative flow during transient
0.00	21.5	0.90	1153.2	No
0.10	70.0	2.92	1179.0	No
0.15	98.6	4.11	1191.8	No
0.20	138.2	5.76	1204.4	Yes
0.50	369.2	15.38	1282.7	Yes
1.00	897.3	37.39	1418.0	Yes
1.25	1200.0	50.00	1486.0	Yes
1.50	1521.7	63.40	1554.0	Yes
1.55	1588.0	66.17	1567.7	Yes

Table 2: Summary of single step reactivity insertions

The results presented in Table 2 were analyzed to establish limits on the amount of reactivity that could be added by a single step insertion without jeopardizing the stability of the system. Also, the total amount of reactivity that could be inserted by making successive single step reactivity insertions without risk was evaluated.

As shown in section 6.1, the step insertion of reactivity may induce a reverse flow (“negative flow”) in the outer fuel assemblies of the core. In order to proceed to a safe restart of the LS-VHTR, no such phenomenon should be observed. Several simulations were run to determine a limit on the inserted reactivity in order to avoid negative flows. It was found that reactivity insertion less or equal to \$0.18 would not induce reverse flow. Thus, no more than \$0.18 reactivity in one step should be added in order to avoid counter-flow.

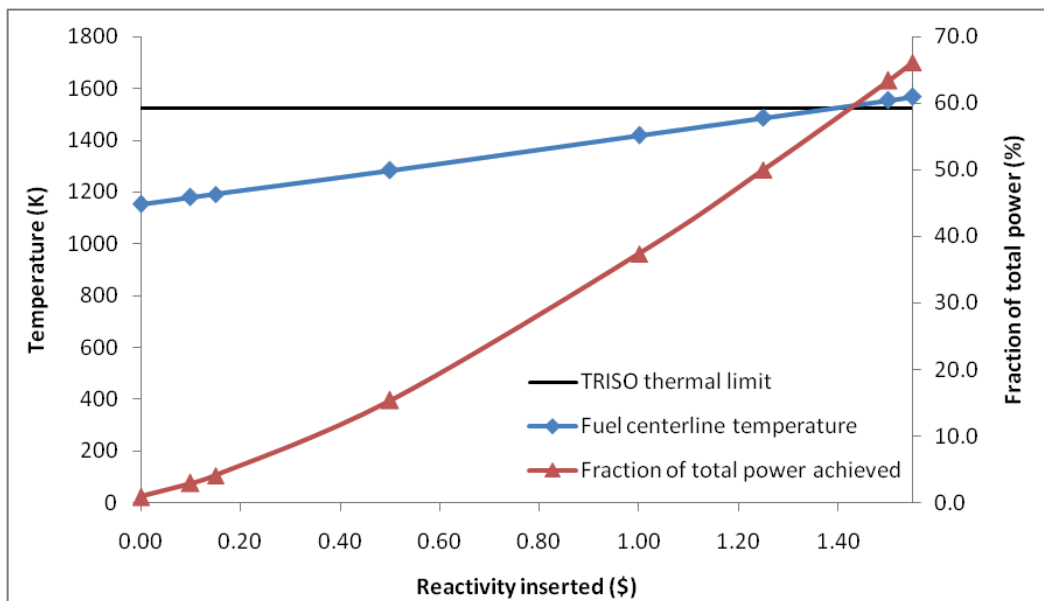


Figure 11: Peak fuel centerline temperature and fraction of total power achieved for 7 different step reactivity insertions

The limit on the fuel temperature was also examined. Current coated TRISO fuel particles offer the capability to operate for long periods at temperatures up to 1523 K (1250°C) [5]. Thus, the total amount of reactivity added to the core by successive step reactivity insertion should not make fuel centerline temperatures hotter than 1523 K. Among the simulations presented in Table 2, the fuel centerline temperature goes past this limit in the \$1.5 insertion case. Additional simulations with different amounts of reactivity inserted in the core were run, in order to study the impact of reactivity insertion on the fuel peak temperature. The maximum fuel temperature and the fraction of total power reached at the end of the transient after adding 7 different amounts of reactivity are shown in Figure 11.

The maximum fuel temperature is below the TRISO thermal limit for a \$1.25 insertion and above the limit for a \$1.5 insertion. The fuel centerline temperature curve intersects the TRISO thermal limit line for inserted reactivity around \$1.40. Thus, the amount of a single step reactivity insertion should remain below this value (plus some safety margin) to preserve the integrity of the TRISO fuel particles.

### 6.3 Potential start-up procedure and simulation

Given the results presented in sections 6.1, 6.2, and the experience of natural circulation power plant start-up from Dodewaard and the ESBWR, a potential start-up procedure for the LS-VHTR with natural circulation of the salt coolant was devised.

It was decided to define a similar kind of start-up, with successive positive step reactivity insertions. Based on the discussion made in the previous section, and in order to prevent any type of instability, it was decided to maintain the insertion of positive reactivity below or at  $\$0.15$ . As mentioned in section 6.2, the fuel temperature should not go past 1523 K in order to preserve the integrity of the TRISO fuel. As a consequence, the amount of successive step insertion was chosen so that the maximum fuel temperature in the core does not exceed that value. The initial reactivity inserted was done at time  $t = 100$  s after the beginning of the simulation. The next insertion was done at time  $t = 2000$  s, and the following insertions were made every 1000 s after this second insertion as shown in Figure 12. The total reactivity inserted with this set of eight  $\$0.15$  reactivity additions was  $\$1.2$ .

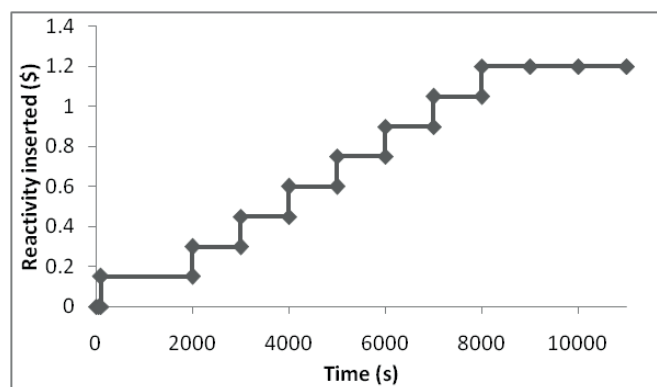


Figure 12: Reactivity insertion curve for the start-up simulation

Figure 13 shows the behavior of the total core reactivity, core power level, decay and fission power, temperature and flow with respect to time during the simulated start-up of the LS-VHTR. It can be observed that during the start-up, the reactivity oscillates between 0 and some positive values. This is due to the fact that a step of positive reactivity is inserted in the core every time that the total reactivity of the core decreases due to the feedback. No negative flow was observed in the outer ring of assemblies during the simulation. The total core mass flow reaches 1713.2 kg/s at the end of the start-up. This flow corresponds to 17.3% of the core mass flow under full power conditions. The core power level goes from 21.5 MW initially to 1138 MW after 18000 s. Thus, with this set of successive reactivity insertions, it takes 2.5 hours to bring the reactor to 47.5% of the total reactor power level.

The core inlet temperature was increased by 10 K while the core outlet temperature increase is 269.7 K. The maximum fuel temperature during the start-up is achieved at the end of the process, with 1472.5 K. This value is 50 K below the limit for preserving the integrity of the coated particles, maintaining this start-up procedure safe regarding fuel temperature.

The results of the start-up simulation showed that no more than 47.5% of the total reactor power level may be reached using natural circulation of the coolant. During the start-up and power increase, it is of course necessary to provide an ultimate heat sink. In order to achieve full power conditions, it is necessary to start generating electricity using the turbines and to restart the circulating pumps at some time during the start-up.

The pumping power required to run the pumps may be calculated using the following equation [20], Eq. (2):

$$P_{\text{pump}} = \frac{\Delta P \times \dot{V}}{0.9} \quad (2)$$

Where  $P_{\text{pump}}$  is the pumping power needed in W,  $\Delta P$  is the pressure drop in Pa, and  $\dot{V}$  is the volumetric flow rate in  $\text{m}^3/\text{s}$ . The denominator 0.9 is used to account for the pump efficiency. The pumping power needed will increase with time since it is proportional to the mass flow. Though, since the rate of the core power increase is greater than the rate of salt flow increase, at some time after the beginning of the start-up the amount of power generated will be sufficient to provide enough electricity to run the pumps. To estimate this time, one should take into account the power conversion efficiency, calculate the electrical power production capability of the reactor at any time during the start-up, and compare that value to the pumping power needed.

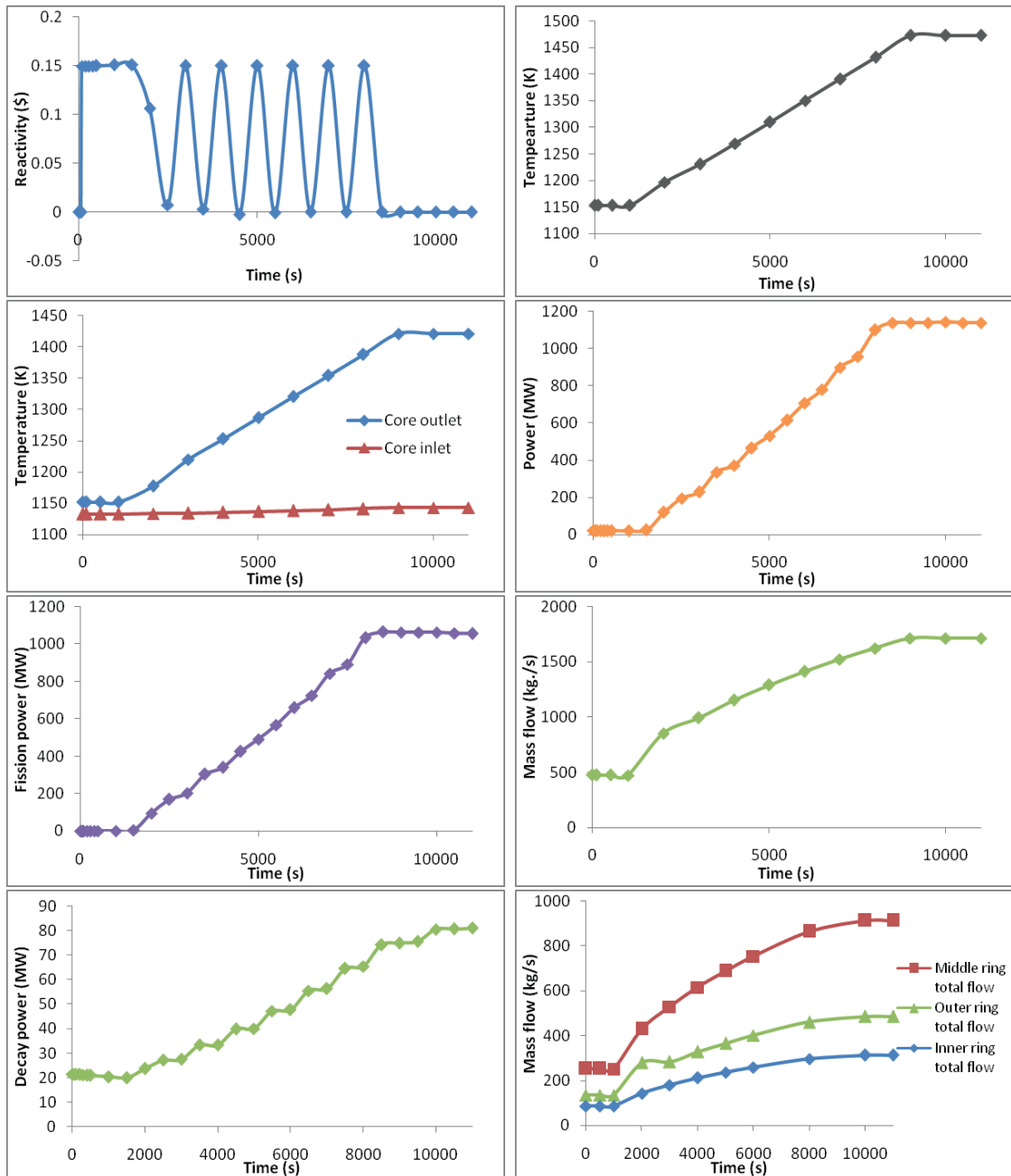


Figure 13: Core reactivity, total power, decay power, fission power, fuel peak temperature, core outlet and inlet temperatures, mass flow rate, and flow in the different rings over time

At the end of the start-up simulation presented previously, the thermal power is 1472.5 MW, the core mass flow is 0.95 m<sup>3</sup>/s (FLiBe density is assumed to be 1800 kg/m<sup>3</sup>), and the pressure drop is 0.2 MPa. Therefore, the calculated pumping power is 233.3 kWe. Using a thermal efficiency of 0.54, the electrical power generated at the end of the simulation would be 795.15 MWe which is many times more. Thus, the restart of the pumps using the electricity provided by the turbines is not limited by the electricity generation capability.

In real life, power production followed by synchronization to grid would be initiated at much lower power, perhaps 3-5% full power, and the electricity produced would need to provide not only pumping power, but the whole power plant electric needs. However, this was beyond the scope of this study and is left for future research.

## 7 CONCLUSIONS

Neutronic and thermal-hydraulic performance of a LS-VHTR were examined. The purpose of this study was to develop and analyze a start-up procedure for this reactor with natural circulation of the coolant, in order to evaluate its feasibility and stability. A model of the LS-VHTR core was developed using the CSAS6 sequence of the SCALE6.0 package to quantify the reactivity feedback due to changes in the fuel temperature or coolant density. A model of the reactor using ORNL baseline design specifications using the RELAP5 software was also developed to simulate the thermal-hydraulic behavior of the reactor during full power operation, shutdown and start-up, and to determine the core reactivity and power changes during a plant start-up. Simulations were performed to determine a potential start-up procedure for the LS-VHTR with natural convection of the coolant, and then to analyze and evaluate this process.

The neutronic calculations evaluated the negative Doppler coefficient for the reactor under study. It was also shown that a decrease in FLiBe density would lead to a positive reactivity feedback. However, it is essential to point out that the change in reactivity induced by the coolant density feedback is negligible compared to the effect of the fuel temperature feedback, thus making the overall reactivity feedback negative and the LS-VHTR passively safe.

Different step reactivity insertion cases were studied, and showed that inserting more than \$0.15 of reactivity in the LS-VHTR core eight hours after its shutdown from full operating conditions could lead to flow instability in the core. In addition, it was shown that inserting more than \$1.2 in the core would make fuel temperatures exceed the thermal capability of the TRISO particles. A potential start-up trajectory was then devised and simulated. The results obtained showed that the reactor power level can be brought to 47.5% of full power without exceeding the fuel thermal limits, and using natural convection of the primary coolant to transfer the heat generated to the intermediate loop.

It should be taken into account that assumptions were made, and the findings presented in this paper should be observed with an appropriate distance. The RELAP5 code was initially developed to simulate the behavior of systems with water as the coolant and was never validated for LS-VHTR, even if the properties of FLiBe and FLiNaK were subsequently added. Thus, this study only provides an indication about the stability and feasibility of a start-up procedure for the LS-VHTR with natural convection of the salt coolant.

Under the assumptions used in this work, it was shown that a stable procedure could be developed, as the one presented in section 6.3, and that a significant core power could be achieved by inserting reactivity stepwise eight hours after the shutdown of the reactor. Thus, this study demonstrated the potential for a passive start-up of the LS-VHTR. However, additional work is needed in order to get a thorough evaluation of the feasibility of a start-up procedure that would not require any offsite power.

In this study, the thermal-hydraulics modeling focused on the primary loop components. The flow and temperatures in the secondary loop were assumed and entered in the RELAP5 code as boundary conditions. Moreover, the power production loop was not modeled in this study, the



power conversion efficiency was assumed based on ORNL expectations for their LS-VHTR conceptual design, and the power needed for the instrumentation of the plant, for the circulating pumps of the intermediate and power production loop, and for the turbines was not taken into account. To get more realistic results, the modeling of the intermediate loop and of the power production loop should be included in future studies.

## REFERENCES

- [1] U.S. DOE Nuclear Energy Research Advisory Committee. “A Technology Roadmap for Generation IV Nuclear Energy Systems Executive Summary”, March 2003.
- [2] World Nuclear Association. “Nuclear Power in the Netherlands”, <http://www.world-nuclear.org/info/inf107.html>.
- [3] U.S. Nuclear Regulatory Commission. “Design certification application reviews - EBWR”, <http://www.nrc.gov/reactors/new-reactors/design-cert/esbwr/review-schedule.html>.
- [4] D. T. Ingersoll, C. W. Forsberg, P. E. MacDonald. “Trade Studies for the Liquid-Salt-Cooled Very High Temperature Reactor: Fiscal Year 2006 Progress Report”, Oak Ridge National Laboratory, ORNL/TM-2006/140, February 2007.
- [5] D. T. Ingersoll, C. W. Forsberg, L. J. Ott, D. F. Williams, J. P. Renier, D. F. Wilson, S. J. Ball, L. Reid, W. R. Corwin, G. D. Del Cul, P. F. Peterson, H. Zhao, P. S. Pickard, E. J. Parma, M. Vernon. “Status of Preconceptual Design of the Advanced High-Temperature Reactor (AHTR)”, Oak Ridge National Laboratory, ORNL/TM-2004/104, May 2004.
- [6] D. T. Ingersoll. “Status of Physics and Safety Analyses for the Liquid-Salt-Cooled Very High-Temperature Reactor (LS-VHTR)”, Oak Ridge National Laboratory, ORNL/TM-2005/218, December 2005.
- [7] D. E. Holcomb. “Fluoride Salt Cooled High-Temperature Reactors (FHRs), Successor to the LWR?”, Presentation for Georgia Tech Graduate Seminar, Oak Ridge National Laboratory, January 2011.
- [8] L. C. Olson. “Materials Corrosion in Molten LiF-NaF-KF Eutectic Salt”, University of Wisconsin-Madison, 2009.
- [9] D. F. Williams, L. M. Toth, K. T. Clarno. “Assessment of Candidate Molten Salt for the Advanced High-Temperature Reactor (AHTR)”, Oak Ridge National Laboratory, ORNL/TM-2006/12, March 2006.
- [10] S. Goluoglu, D. F. Hollenbach, L. M. Petrie. “CSAS6: control module for enhanced criticality safety analysis with KENO-VI”, Oak Ridge National Laboratory, January 2009.
- [11] D. F. Hollenbach, J. A. Bucholz. “Theoretical background for calculational methods in SCALE”, Oak Ridge National Laboratory, ORNL/TM-2005/39, January 2009.
- [12] The RELAP5-3D Code Development Team. “RELAP5-3D© Code manual volume I: code structure, system models, and solution methods”, Idaho National Laboratory, INEEL-EXT-98-00834, June 2005.

- [13] RSICC. "SCALE code package", <http://www-rsicc.ornl.gov/codes/ccc/ccc7/ccc-750.html>.
- [14] D. F. Hollenbach, L. M. Petrie, S. Goluoglu, N. F. Landers, M. E. Dunn. "KENO-VI: a general quadratic version of the KENO program", Oak Ridge National Laboratory, ORNL/TM-2005/39, January 2009.
- [15] C. B. Davis. "Implementation of Molten Salt Properties into RELAP5-3D/ATHENA", Idaho National Laboratory, September 2005.
- [16] The RELAP5-3D© Code Development Team. "RELAP5-3D© Code Manual Volume II: User's Guide and Input Requirements / Appendix A RELAP5-3D© Input Data Requirements", Idaho National Laboratory, INEEL-EXT-98-00834-V2, 2005.
- [17] P. E. MacDonald. "NGNP Preliminary Point Design - Results of Initial Neutronics and Thermal-Hydraulic Assessment During FY-03", Idaho National Engineering and Environmental Laboratory, INEEL/EXT-03-00870, 2003.
- [18] Haynes International Inc. "HASTELLOY® N alloy", 2002.
- [19] J. J. Duderstadt, L. J. Hamilton. "Nuclear Reactor Analysis", WILEY Interscience, 1976.
- [20] D. E. Holcomb, D. Ilas, V. K. Varma, A. T. Cisneros, R. P. Kelly, J. C. Gehin. "Core and refueling design studies for the advanced high temperature reactor", Oak Ridge National Laboratory, ORNL/TM-2011/365, September 2011.